Journal of Solid State Chemistry 186 (2012) 231–234

Contents lists available at SciVerse ScienceDirect

Journal of Solid State Chemistry

journal homepage: www.elsevier.com/locate/jssc

Structural phase transitions of SrF_2 at high pressure

J.S. Wang [a,b], C.L. Ma [a], D. Zhou [a], Y.S. Xu [a], M.Z. Zhang [a], W. Gao [a], H.Y. Zhu [a], Q.L. Cui [a,*]

[a] State Key Laboratory of Superhard Materials, Jilin University, Changchun 130012, PR China
[b] Jilin Normal University, Siping 136000, PR China

ARTICLE INFO

Article history:
Received 11 July 2011
Received in revised form
2 November 2011
Accepted 11 December 2011
Available online 22 December 2011

Keywords:
SrF_2
Synchrotron radiation
Phase transition
Bulk modulus

ABSTRACT

The high-pressure behavior of SrF_2 has been investigated by angle-dispersive synchrotron X-ray powder diffraction measurement up to 50.3 GPa at room temperature. Two phase transformations were observed at 6.8 and 29.5 GPa, and the two high pressure phases were identified as orthorhombic (*Pnma*) phase and hexagonal ($P6_3/mmc$) phase by Rietveld refinement. Upon decompression, retransformation was observed and the sample recovered under ambient conditions consisted of a mixture of cubic phase and orthorhombic phase. The compressing characteristics of SrF_2 as the pressure increases were discussed, indicating higher incompressibility of SrF_2 under high pressure.

1. Introduction

The alkaline earth fluorides are an important class of materials that form the basis of a range of applications such as geosciences, materials science, and condensed-matter physics [1,2]. In terms of the applications, the alkaline earth fluorides have attracted considerable interest due to their unique properties, including low-energy phonons, high ionicity, electron-acceptor behavior, high resistivity, and anionic conductivity [3–5]. Since fluorides are more compressible, phenomena involving large lattice strains can be observed over a relatively narrow pressure range. They have been used as mineralogical models for the behavior of ionically bonded minerals in the Earth's mantle and as test materials for the development of high-pressure equations of state [6]. Therefore, the pressure-dependent properties of alkaline earth fluorides are of considerable interest in a number of applied and fundamental respects.

At ambient conditions, SrF_2 crystallizes in the cubic fluorite structure with a space group of $Fm3m$, which consists of a cubic close-packed array of cations with anions occupying tetrahedral sites. According to a large number of research carried out on CaF_2 and BaF_2, the sequence of the pressure-induced phase transition would follow the structural progression from cubic ($Fm3m$) fluorite structure to orthorhombic (*Pnma*) cotunnite-type structure to hexagonal ($P6_3/mmc$) Ni_2In-type structure, which in turn would be characterized by a progression in the cation coordination number from 8 to 9 to 11. Despite there are many high-pressure studies on CaF_2 [7–11] and BaF_2 [12–15], as an important kind of alkaline earth metal fluoride, very little experimental and theoretical works have been reported the structural stabilities of SrF_2. Earlier Raman spectra and theoretical studies [16–18] showed that the first-order phase transformation from the cubic to orthorhombic phase transition occurs in the pressure range of 4–7 GPa. Recently, the second phase transition from orthorhombic phase to hexagonal phase at about 46 GPa has been predicted [19]. In addition, Dorfman et al. [1] observed that the orthorhombic phase transformed to the hexagonal phase upon compression at 36 GPa with heating to about 1500 K. To our knowledge, few high-pressure studies either theoretical or experimental have been reported to investigate the structural phase transition of SrF_2 at room temperature, especially for the second phase transition from orthorhombic phase to hexagonal. Theoretical predictions of phase-transition pressures and bulk moduli for the high-pressure phases span a wide range, but lacking of enough experimental data to identify the high-pressure behavior of SrF_2. Therefore, an accurate investigation of the structural change of SrF_2 under pressure at room temperature is highly required.

We studied the high-pressure behavior of SrF_2 up to 50.3 GPa at room temperature using *in situ* angle-dispersive X-ray diffraction (ADXD) measurement. The high pressure phases were identified by Rietveld refinement. The phase stability, structure, atomic positions and bulk modulus of SrF_2 are compared and analyzed in detail.

2. Experimental details

Powder sample of SrF_2 (99.99%) was obtained from Alfa Aesar. X-ray diffraction confirmed that it is in the fluorite-type structure. The lattice constant at atmospheric pressure, a_0, has been

* Corresponding author. Fax: +86 431 8516 8346.
E-mail address: cql@jlu.edu.cn (Q.L. Cui).

0022-4596/$ - see front matter © 2011 Elsevier Inc. All rights reserved.
doi:10.1016/j.jssc.2011.12.015

determined to be 5.810(2) Å, which is consistent with the value of a_0=5.800 Å (PDF Card No. 06-0262). The sample powder was loaded into a gasketed high-pressure Mao-Bell-type diamond anvil cell (DAC) with 400 μm culet diamond anvils. A 100-μm-diameter hole was drilled through the center of a preindented 60-μm-thick T-301 stainless steel gasket to form a sample chamber. SrF_2 is sensitive to moisture, in order to avoid hydrolyzing, selecting silicone grease as the pressure transmitting medium. Pressure was determined from the frequency shift of the ruby R1 fluorescence line [20].

ADXD experiments were carried out up to 50.3 GPa at room temperature using a synchrotron X-ray source (λ=0.485946 Å) of the B2 High-Pressure Station of Cornell High Energy Synchrotron Source (CHESS). The diffraction data were collected using MAR165 CCD detector. The two-dimensional X-ray diffraction (XRD) images were analyzed using the FIT2D software, yielding one-dimensional intensity versus diffraction angle 2θ patterns. The average acquisition time for each X-ray diffraction pattern was 400 s. The sample–detector distance and geometric parameters were calibrated using a CeO_2 standard. High-pressure synchrotron XRD patterns were fitted by Rietveld profile matching using the MATERIAL STUDIO program.

3. Results and discussion

3.1. X-ray diffraction

Fig.1 shows X-ray diffraction patterns for SrF_2 collected by increasing the pressure gradually up to 50.3 GPa. With increasing pressure, the diffraction lines shift toward higher 2θ angles accompanied by a change of the relative intensities. Fig.2 shows Rietveld full-profile refinements of the diffraction patterns collected on compression at 1.2, 15.2, and 44.4 GPa, respectively. The Rietveld refinement of SrF_2 performed at 1.2 GPa (Fig.2a) shows a good agreement with the cubic structure with a lattice constant of 5.768(3) Å. At 6.8 GPa, new diffraction peaks start to appear in the XRD patterns, indicating an occurrence of the phase transition, and the volume change for the coexistence of cubic and orthorhombic phases is a decrease of 9.3% from the low-pressure phase. With increasing pressure to 15.2 GPa, additional diffraction peaks assigned to the high-pressure phase arise, and in the meantime all

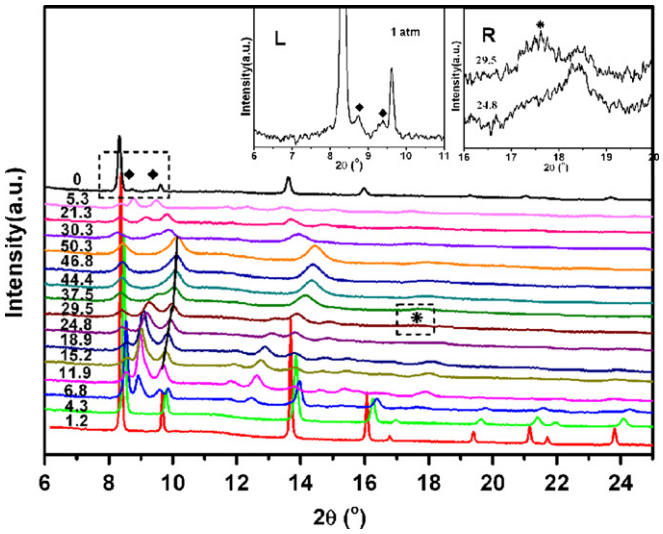

Fig. 1. Angle dispersive XRD patterns of SrF_2 at selected pressures at room temperature. Diamond indicates the orthorhombic phase diffraction peaks. Asterisk indicates the hexagonal phase diffraction peak. The insets show enlarged areas of the diffraction patterns to illustrate the appearance of weak peaks.

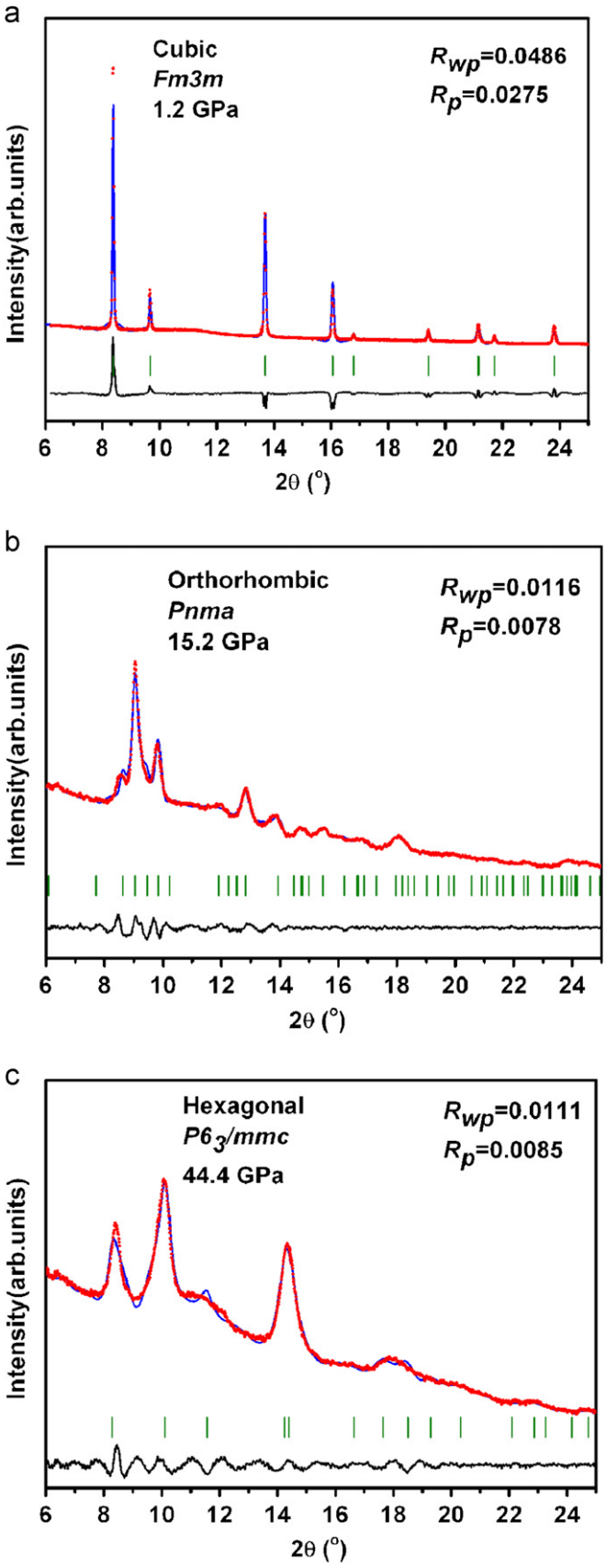

Fig. 2. Rietveld full-profile refinements of the diffraction patterns collected on compression at (a) 1.2 GPa, (b) 15.2 GPa, and (c) 44.4 GPa. Dots, upper, and lower solid lines represent experimental, calculated, and residual patterns, respectively. Bars are marked at the positions of diffraction peaks.

Table 1
Lattice Constants and refined fractional coordinates for the *Fm*3*m*, *Pnma*, and $P6_3/mmc$ phase of SrF_2.

Symmetry	Lattice parameters (Å)	Atom	Atomic positions		
			x	*y*	*z*
Cubic (1.2 GPa)	$a=5.768(3)$	Sr(4a)	0	0	0
		F(8c)	1/4	1/4	1/4
Orthorhombic	$a=6.154(5)$	Sr(4c)	0.254(3)	0.117(4)	0.25
(15.2 GPa)	$b=7.312(3)$	F1(4c)	0.482(9)	0.497(3)	0.25
	$c=3.645(1)$	F2(4c)	0.989(6)	0.723(5)	0.25
Hexagonal	$a=3.841(1)$	Sr(2c)	1/3	2/3	1/4
(44.4 GPa)	$c=4.783(8)$	F1(2a)	0	0	0
		F2(2d)	1/3	2/3	3/4

diffraction peaks from the cubic phase disappear, which means the cubic phase completely transformed into orthorhombic phase. Fig.2b presents the Rietveld refinement of SrF_2 performed at 15.2 GPa, showing good agreement with a orthorhombic cell with space group *Pnma* with lattice parameters $a=6.154(5)$ Å, $b=7.312(3)$ Å, and $c=3.645(1)$ Å. The unit-cell parameters and atomic positions of the high-pressure phase are given in Table 1.

At 29.5 GPa, a new diffraction peak marked with asterisk begins to emerge, and the new peak is enlarged as shown in graph labeled R (inset in Fig.1). With the pressure further increasing, all diffraction peaks shift toward higher angles. However, a discontinued shift is strikingly observed around 29.5 GPa. At the same time, some peaks from the cotunnite-type phase turn to be fairly weak and finally vanish at 44.4 GPa. The variation of the ADXD pattern indicates a second phase transition of SrF_2 begins at 29.5 GPa and completes at 44.4 GPa. Fig.2c presents the Rietveld refinement of SrF_2 performed at 44.4 GPa, showing good agreement with a hexagonal cell with space group $P6_3/mmc$ with lattice parameters $a=3.841(1)$ Å and $c=4.783(8)$ Å (Table 1).

Several pressure-induced phase transitions in CaF_2 and BaF_2 have recently been reported. In the case of CaF_2, a sequence of structural transformations along the path fluorite→cotunnite→Ni_2In-type occurs at pressures of about 9.5 and 72 GPa, respectively [4,8]. In BaF_2, two phase transitions were characterized at 3 and 14 GPa, respectively [8,12]. The present and previous studies on CaF_2, SrF_2, and BaF_2 show that the compounds with heavier elements, going down the IIA column of the periodic table, tend to adopt low phase-transition pressures. This result is in excellent agreement with the high-pressure behaviors of the alkali-metal sulfides reported by Santamaría-Pérez et al. [21,22].

The transition pressure to the Ni_2In-type structure is lower than theoretical prediction about 46 GPa [19]. The Ni_2In-type structure is a subgroup of the cotunnite-type structure with an ideal hcp anion lattice. In the theoretical calculations, the energy difference is very small between the *Pnma* and the $P6_3/mmc$ phase. Therefore the parameter used in theoretical calculation has tremendous influence on the calculation result. It may be the mainly reason causing the transition pressure difference between theoretical and experimental results. Such a small energy difference would also increase the dependence of experimental results on temperature, differential stress, and kinetics [1].

Upon decompression, the orthorhombic high-pressure phase is recovered when the pressure is released down to 30.3 GPa. The experimental data point that the transition from orthorhombic to cubic phase exhibits strong hysteresis under decompression. After decompression to ambient condition, the sample reverts back to the fluorite structure with a few peaks attributed to orthorhombic cotunnite-type structure. It indicates that the cubic and orthorhombic phase co-exist at the ambient pressure. In Ref. [16], the cubic structure is recovered when pressure is released down to 1.4 GPa, and the orthorhombic phase has not been retained. However, it was stated that the phase transformation is irreversible even when the sample was quenched to atmospheric pressure [23]. This is contrary to the observation which was reported in Ref. [16].In fact, the previous research shows that the pressure environment could be responsible for the hysteresis of high pressure phase [24]. The shear stress presents in DAC experiment could lead to irreversibility after complete pressure release. However, the current experiments used silicone grease as the pressure-transmitting medium. There is no shear stress created in the silicone grease medium at low pressure (below 10 GPa) and it is hydrostatic [25]. Therefore, the hysteresis cannot be attributed to the pressure-transmitting medium, which might be explained as the inherent sluggish nature of SrF_2. The residual stress in sample is not completely released upon decompression, which might be the reason of irreversibility at the ambient pressure.

3.2. Equation of state

The bulk modulus B_0 and its pressure derivative B_0' of each phase of SrF_2 were derived by a least squares fitting of the data shown in Fig. 3 with the Birch–Murnaghan equation [26]:

$$P=(3/2)B_0[(V/V_0)^{-7/3}-(V/V_0)^{-5/3}]\{1+(3/4)(B_0'-4)\times[(V/V_0)^{-2/3}-1]\}$$

where V and V_0 denote the volumes at pressure P and ambient pressure, respectively. Values of B_0 and B_0' derived are shown in Table 2, as well as other experimental and calculated data. Alternatively, B_0' may be fixed to a reasonable value based on previous work. The bulk modulus value of fluorite SrF_2 is 73(3) GPa with B_0' fixed at 4, in good agreement with the previous works [18,19,27,28]. With B_0' fixed at 4.7, we yield $B_0=85(5)$ GPa for the cotunnite-type phase and 99(10) GPa for the Ni_2In-type phase, respectively. The isothermal bulk modulus of cotunnite-type phase at ambient pressure is higher than the fluorite phase. For the cotunnite-Ni_2In transition, there is significantly increase in bulk modulus obtained in this work (Table 2). However, the bulk modulus value of Ni_2In-type phase measured by theoretical calculation (44 GPa) is considerably smaller than the current experiment. In previous experimental and theoretical studies on the Ni_2In-type phase of BaF_2 [29,30], the bulk modulus is also

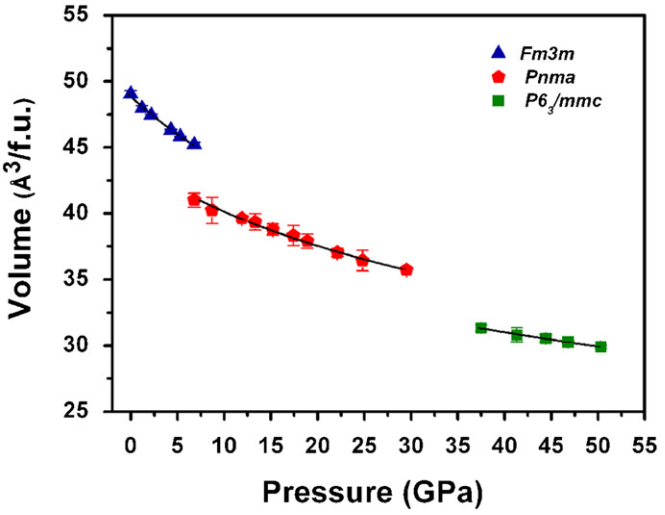

Fig. 3. The volumes per formula unit of the various phases of SrF_2 as a function of pressure at room temperature. Solid curves are the Birch–Murnaghan EOS fits to the experimental data (error bars shown when they exceed size of data points) in this study.

Table 2
Birch–Murnaghan EOS parameter values for fluorite, cotunnite, and Ni_2In-type structures of SrF_2 from this and previous studies.

	Fm3m		*Pnma*		*P6$_3$/mmc*	
	Theoretical	Experimental	Theoretical	Experimental	Theoretical	Experimental
B_0(GPa)	66.2 [19] 90.4 [18] 64.2 [17] 67.8 [28]	69 [27] 73(3)	117 [19] 127 [18] 99.4 [17]	74(8) [1] 85(5)	43.8 [19]	125(9) [1] 99(10)
B_0'	–	4	–	4.7	–	4.7

obviously higher than cotunnite-type phase. Our results are consistent with previous studies on bulk modulus of BaF_2. The increased bulk modulus at high pressure indicates higher incompressibility of the high-pressure phase of SrF_2.

Bulk modulus of Ni_2In-type phase yielded in this work is lower than that reported by Dorfman et al. [1]. The large distinction between two works may be induced by the different conditions of two experiments. The two works selected different pressure transmitting medium. In Dorfman et al.'s experiment, they selected the solid pressure transmitting media, and the SrF_2 sample was measured at high temperature. However, the current experiment used a liquid pressure transmitting medium and performed at ambient temperature. Therefore, it is understandable that this work yielded lower bulk modulus for Ni_2In-type phase.

4. Conclusion

In summary, we experimentally confirm static pressure-induced structural phase transitions of SrF_2 using synchrotron radiation XRD at room temperature. Under pressures up to 50.3 GPa, SrF_2 transforms from the cubic fluorite structure to an orthorhombic cotunnite-type structure at about 6.8 GPa and then to a hexagonal Ni_2In-type structure at 29.5 GPa, consistent with the previously studied phase transition sequence on Ca/BaF_2. The three stable structures are confirmed by Rietveld refinements of the X-ray diffraction data. After decompression to ambient condition, the some peaks attributed to orthorhombic phase have been retained, suggesting that the cubic and orthorhombic phase co-exist at ambient pressure. The isothermal bulk modulus of the cubic, orthorhombic, and hexagonal phases increased gradually, indicating higher incompressibility of SrF_2 under high pressure.

Acknowledgments

This work was supported financially by the National Natural Science Foundation of China (No. 11074089) and the National Basic Research Program of China (2011CB808200). Cornell High Energy Synchrotron Source (CHESS) is supported by NSF and NIH/NIGMS through a NSF award DMR-0936384.

References

[1] S.M. Dorfman, F. Jiang, Z. Mao, A. Kubo, Y. Meng, V.B. Prakapenka, T.S. Duffy, Phys. Rev. B 81 (2010) 174121.
[2] A. Bensalaha, M. Mortiera, G. Patriarcheb, P. Gredinc, D. Vivien, J. Solid. State. Chem. 179 (2006) 2636–2644.
[3] C. Feldmann, M. Roming, K. Trampert, Small 2 (2006) 1248–1250.
[4] Z.W. Quan, D.M. Yang, P.P. Yang, X.M. Zhang, H.Z. Lian, X.M. Liu, J. Lin, Inorg. Chem. 47 (2008) 9509–9517.
[5] P. Gao, Y. Xie, Z. Li, Eur. J. Inorg. Chem. 16 (2006) 3261–3265.
[6] A. Kavner, Phys. Rev. B 77 (2008) 224102.
[7] X. Wu, S. Qin, Z.Y. Wu, Phys. Rev. B 73 (2006) 134103.
[8] L. Gerward, J.S. Olsen, S. Steenstrup, S.A. Sbrink, A. Waskowska, J. Appl. Crystallogr. 25 (1992) 578–581.
[9] E. Morris, T. Groy, K. Leinenweber, J. Phys. Chem. Solids 62 (2001) 1117–1122.
[10] S.E. Boulfelfel, D. Zahn, O. Hochrein, Y. Grin, S. Leoni, Phys. Rev. B 74 (2006) 094106.
[11] K.F. Seifert, Ber. Bunsenges. Phys. Chem. 70 (1966) 1041.
[12] J.S. Smith, S. Desgreniers, J.S. Tse, J. Sun, D.D. Klug, Y. Ohishi, Phys. Rev. B 79 (2009) 134104.
[13] H.I. Smith, J.H. Chen, Bull. Am. Phys. Soc 11 (1966) 414.
[14] K.F. Seifert, Fortschr .Miner. 45 (1967) 214.
[15] J.R. Kessler, E. Monberg, M. Nichol, J. Chem. Phys. 60 (1974) 5057–5065.
[16] G.A. Kourouklis, E. Anastassakis, Phys. Rev. B 34 (1986) 1233.
[17] E. Francisco, M.A. Blanco, G. Sanjurjo, Phys. Rev. B 63 (2001) 094107.
[18] V. Kanchana, G. Vaitheeswaran, M. Rajagopalan, Physica B 328 (2003) 283–290.
[19] A.M. Hao, X.C. Yang, J. Li, W. Xin, S.H. Zhang, X.Y. Zhang, R.P. Liu, Chin. Phys. Lett. 26 (2009) 077103.
[20] H.K. Mao, J. Xu, P.M. Bell, J. Geophys. Res. 91 (1986) 4673–4676.
[21] D. Santamaría-Pérez, A. Vegas, C. Muehle, M. Jansen, Acta Cryst. B67 (2011) 109–115.
[22] D. Santamaría-Pérez, A. Vegas, C. Muehle, M. Jansen, J. Chem. Phys. 135 (2011) 054511.
[23] D.P. Dandekar, J.C. Jamieson, Trans. Am. Crystallogr. 5 (1969) 19–27.
[24] D. Errandonea, Y. Meng, M. Somayazulu, D. Haüsermann, Physica B 355 (2005) 116–125.
[25] Y. Shen, R.S. Kumar, M. Pravica, M.F. Nicol, Rev. Sci. Instrum. 75 (2004) 4450–4454.
[26] F. Birch, J. Geophys. Res. 83 (1978) 1257.
[27] G.A. Samara, Phys. Rev. B 13 (1976) 4529.
[28] M. M'erawa, M. Llunell, R. Orlando, M. Gelize-Duvignau, R. Dovesi, Chem. Phys. Lett. 368 (2003) 7–11.
[29] J.M. Léger, J. Haines, A. Atouf, Phys. Rev. B 51 (1995) 3902–3905.
[30] V. Kanchana, G. Vaitheeswaran, M. Rajagopalan, J. Alloys. Compd. 359 (2003) 66–72.